

## Radar and Damage Analysis of Severe Bow Echoes Observed during BAMEX

DUSTAN M. WHEATLEY AND ROBERT J. TRAPP

*Purdue University, West Lafayette, Indiana*

NOLAN T. ATKINS

*Lyndon State College, Lyndonville, Vermont*

(Manuscript received 31 January 2005, in final form 22 June 2005)

### ABSTRACT

This study examines damaging-wind production by bow-shaped convective systems, commonly referred to as bow echoes. Recent idealized numerical simulations suggest that, in addition to descending rear inflow at the bow echo apex, low-level mesovortices within bow echoes can induce damaging straight-line surface winds. In light of these findings, detailed aerial and ground surveys of wind damage were conducted immediately following five bow echo events observed during the Bow Echo and Mesoscale Convective Vortex (MCV) Experiment (BAMEX) field phase. These damage locations were overlaid directly onto Weather Surveillance Radar-1988 Doppler (WSR-88D) images to (i) elucidate where damaging surface winds occurred within the bow-shaped convective system (in proximity to the apex, north of the apex, etc.), and then (ii) explain the existence of these winds in the context of the possible damaging-wind mechanisms.

The results of this study provide clear observational evidence that low-level mesovortices within bow echoes can produce damaging straight-line winds at the ground. When present in the BAMEX dataset, mesovortex winds produced the *most* significant wind damage. Also in the BAMEX dataset, it was observed that smaller-scale bow echoes—those with horizontal scales of tens of kilometers or less—produced more significant wind damage than mature, extensive bow echoes (except when mesovortices were present within the larger-scale systems).

### 1. Introduction

Our understanding of the mechanisms that produce severe winds within bow echoes is the culmination of several inquiries in severe storms research. Early studies by Nolen (1959) and Hamilton (1970) recognized the severe weather potential of bulging radar echo configurations. Fujita (1978) provided the first conceptual representation of the structure and evolution of severe bow echoes. In Fujita's conceptual model, as considered from a radar perspective, a strong, tall echo transitions to a bow echo under the influence of intense downdrafts near the bow echo apex. Later studies (Smull and Houze 1987; Jorgensen and Smull 1993; see also Fujita 1978) further clarified the kinematic structure of bow echoes by documenting the presence of a

midlevel, rear-inflow jet (RIJ). Descending rear inflow at the bow echo apex has traditionally been considered to be the primary cause of damaging winds near the ground; microbursts have also been shown to produce more localized areas of damage within bow echoes (e.g., Forbes and Wakimoto 1983).

Recent idealized numerical simulations suggest an evolving conceptualization. Specifically, Trapp and Weisman (2003) found that the *most* damaging winds in mature, extensive bow echoes can be induced by low-level (altitudes  $\leq 1$  km AGL), meso- $\gamma$ -scale ( $\sim 10$  km) vortices, or "mesovortices," located tens of kilometers northwest of the bow echo apex (along the leading edge of the system). These circulations form at low levels as crosswise horizontal baroclinic vorticity is tilted vertically by downdrafts. On a time scale less than an hour, the resultant vortex couplet gives way to a dominant cyclonic vortex, due in part to the vertical stretching of planetary vorticity. Intense, near-ground winds are driven by the low-level mesovortex circulation, as revealed by an analysis of forcing terms in the horizontal

---

*Corresponding author address:* Dr. Robert J. Trapp, Department of Earth and Atmospheric Sciences, Purdue University, 550 Stadium Mall Drive, West Lafayette, IN 47907.  
E-mail: jtrapp@purdue.edu

momentum equations. Notably, the wind damage pattern associated with these vortices would be “straight line” (i.e., nontornadic) in appearance, a consequence of their size and asymmetry.

As found in the idealized experiments of Trapp and Weisman (2003), low-level mesovortices are especially favored in environments characterized by moderate to strong low-level unidirectional vertical wind shear ( $\geq 15 \text{ m s}^{-1}$  over the lowest 2.5 km AGL) and large instability (e.g., CAPE greater than  $\sim 2000 \text{ J kg}^{-1}$ ; Weisman and Trapp 2003). Under these conditions, the midlevel RIJ remains elevated until descending near the leading edge of the system, which confines RIJ-associated winds to a narrow band in proximity to the apex. Thus, the numerical results suggest that mesovortex winds can be more intense, have longer duration, and instantaneously affect a larger area than RIJ/apex winds. Bow echoes simulated in weaker shear regimes possess weaker, shallower, and shorter-lived mesovortices.

Low-level mesovortices have been shown frequently in observations (e.g., Funk et al. 1999; Schmocker et al. 2000; Wolf 2000); however, the corroborative observational data that clearly differentiates low-level mesovortex from RIJ-associated winds is limited. At present, only a few observational studies in the informal literature have indirectly or directly documented the role of mesovortices in the production of damaging surface winds within bow echoes. Miller and Johns (2000) investigated several long-lived mesoscale convective systems (MCSs) that produced “extreme” damaging wind, tantamount in this case to upper-F1-intensity damage. One such system, a bow echo event on 4 July 1999, caused a widespread tree blowdown in northern Minnesota. Markedly, this wind damage occurred beneath what they referred to as a supercell embedded within the northern flank of the system. Wind damage in proximity to the apex was less dense, with only pockets of extreme wind damage.

Wolf’s (2000) analysis of the early formation of the bow echo event on 29 June 1998 revealed six subsystem-scale, cyclonic vortices along the leading edge of the convective system, five of which were nontornadic (see also Atkins et al. 2004). All of the vortices formed in proximity to or north of the bow echo apex, and were in general short-lived (lasting only a few radar volume scans). While the convective event produced widespread, F0-intensity wind damage across eastern Iowa and central Illinois, localized swaths of F1-intensity wind damage were found to occur in association with the cores of the nontornadic circulations. Similar relations between vortex tracks and point observations were noted by Przybylinski et al. (2000) and Schmocker et al. (2000). An indirect role of *midlevel* vortices in the

production of damaging straight-line winds has been suggested by Cotton et al. (2003).

The results of the studies summarized above indicate the need to revisit the established conceptual model and delve deeper into hypothesized ideas of damaging-wind production within bow echoes. New data needed to do so, specifically, from detailed post-storm damage surveys, have recently become available through the auspices of the Bow Echo and Mesoscale Convective Vortex (MCV) Experiment (BAMEX; Davis et al. 2004). Using a straightforward technique that couples damage survey data with complementary Doppler radar scans, we aim herein to

- 1) elucidate where damaging surface winds occurred within the bow-shaped convective system (in proximity to the apex, north of the apex, etc.), and then
- 2) explain the existence of these winds in the context of the possible damaging-wind mechanisms.

In section 2, the data sources are described, followed by a discussion of the research methodology employed in this study. In sections 3–6, each of five bow echo events is described in detail, using complementary radar-damage analyses. Finally, in section 7, the results of this study are summarized, their implications are discussed, and suggestions for future research on this topic are offered.

## 2. Methodology

This study considers the possible mechanism(s) of damaging-wind production in five bow echo events (Table 1)<sup>1</sup> observed during the BAMEX field phase, which was conducted from 20 May–6 July 2003 over an experimental domain that encompassed the Midwest, upper Ohio River Valley, and parts of the Great Plains. Although a number of special airborne and ground-based observing instruments were deployed during BAMEX (see Davis et al. 2004), our two objectives required only post-event damage surveys and the existing Weather Surveillance Radar-1988 Doppler (WSR-88D) network.

### a. Damage survey techniques

As also described in a companion paper by Atkins et al. (2005), detailed aerial and ground surveys of wind

---

<sup>1</sup> The term “cell bow echo” originates from the work of Lee et al. (1992) and is used to describe bow systems with horizontal scales of 10–25 km. The term “bow echo” is used to describe bow systems with horizontal scales of 60–100 km (or greater). The latter may occur as an isolated phenomenon, or as part of a larger quasi-linear convective system.

TABLE 1. Summary of BAMEX damage surveys included in this study.

Date(s)	Mode	Location	Aerial survey	Ground survey
31 May	MCS	Wingate, IN	Atkins	Trapp
10 Jun	Cell bow echo	Emerson, NE	Atkins	Wheatley
10 Jun	Cell bow echo	Shelby, NE	Atkins	Wheatley
4–5 Jul	Bow echo	Indiana/Ohio	None	Trapp, Wheatley
5–6 Jul	Bow echo	Nebraska/Iowa	Atkins, Wakimoto	Atkins, Wakimoto

damage were conducted by the authors and other BAMEX personnel (see Table 1) immediately following apparently severe bow echo events. These surveys were critical in characterizing the damaging surface winds within severe bow echoes, especially because conventional surface observations are sparse relative to the scale of damaging winds. *Storm Data* reports also have been shown to be too sparse (Trapp et al. 2004) and uncertain (e.g., Witt et al. 1998) for the purposes of this study, although we used them to enhance our surveys when appropriate.

The scope of ground and aerial surveys was guided by initial storm reports sent to National Weather Service (NWS) offices and also by Doppler radar imagery. For most events that occurred over an expansive geographic area, aerial surveys were flown using Cessna aircraft to photo-document the scale and intensity of the wind damage. This type of survey facilitated the most comprehensive post-event assessment of the damaging surface winds within a severe bow echo, and provided “right of entry” to those areas (private property, etc.) inaccessible from the existing road network. Further, aerial surveying was advantageous in discerning convergence/divergence patterns associated with tornadic and “straight line” winds, respectively. For completeness, a ground survey team also was deployed immediately following bow echo events of interest. While this type of survey was constrained by the existing road network, it often yielded information about damage intensity that was not evident from the air.

It should be noted that even these special surveys have limitations. As stated, initial survey efforts focused primarily on the areas highlighted in the first storm reports to NWS offices. Expanded survey efforts followed from assessment of these areas, so it is conceivable that unreported damage areas failed to be included in this study. Nonetheless, for reasons already discussed, this approach was favored over a complete dependence upon *Storm Data* reports.

All damage locations were superimposed on high-resolution (1:250 000) U.S. Geological Survey (USGS) topographic maps. “Damage vectors” were used to denote the direction of tree fall and/or the direction in which structural damage was strewn. In some instances,

a direction could not be determined due to cleanup efforts that occurred in the days following the event; these damage locations were denoted simply with a point. Variations of this convention are otherwise noted on a case-by-case basis.

The damage information collected during each survey effort was synthesized into a comprehensive damage analysis, which provides a quantitative description of the (geographical) scale and intensity of the wind damage. Similar to damage analyses of isolated tornadic thunderstorms, the wind speed at each location was assessed in accordance with the Fujita damage intensity scale (Fujita 1981).

#### b. Single-Doppler radar data

The radar data used in this study were obtained from the National Climatic Data Center (NCDC) WSR-88D archive level II dataset, comprised of reflectivity, mean radial velocity, and spectrum width over full volumetric scans. Single-Doppler radar observations were incorporated in the present study from the following WSR-88D sites across the Midwest: Wilmington, Ohio (KILN); Indianapolis, Indiana (KIND); North Webster, Indiana (KIWX); and Omaha, Nebraska (KOAX). The WSR-88D data were preprocessed using the software program SOLO (Oye et al. 1995). The Mesocyclone Detection Algorithm<sup>2</sup> (MDA; Stumpf et al. 1998) included in the research version of Warning Decision Support System–Integrated Information (WDSS–II; Lakshmanan 2002; Stumpf et al. 2002) was utilized to facilitate the identification and diagnosis of mesovortices.

To ensure an accurate comparison between geographic locations defined by the radar data and surveys, it was highly desirable to check the accuracy of range and azimuth measurements of these single-Doppler ra-

<sup>2</sup> Although the low-level mesovortices in these BAMEX cases had a range of sizes, strengths, and depths, most were identified at some point as mesocyclones by the MDA. As described in Stumpf et al. (1998), the (now WSR-88D) mesocyclone criteria include a velocity difference ( $\Delta v$ ) threshold of  $30 \text{ m s}^{-1}$  and a shear threshold of  $5 \text{ m s}^{-1} \text{ km}^{-1}$ . The thresholds are relaxed linearly to 75% for  $\Delta v$  and 50% for shear within the range 100–200 km, and held constant beyond 200 km.



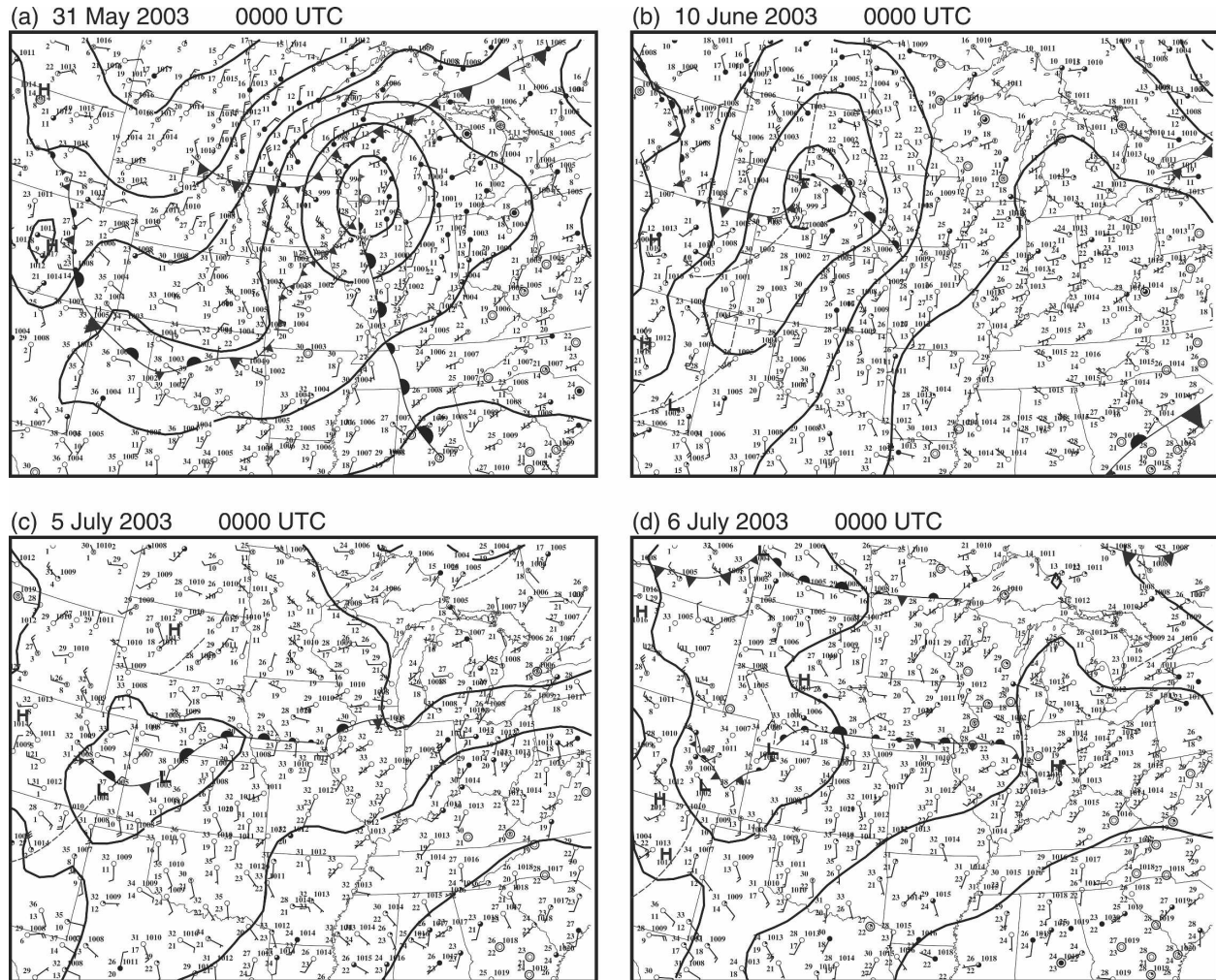


FIG. 1. Analysis of surface mean sea level pressure (solid contours; 4-hPa increment), valid 0000 UTC on (a) 31 May 2003, (b) 10 Jun 2003, (c) 5 Jul 2003, and (d) 6 Jul 2003. Full and half wind barbs denote wind speeds of 5 and  $2.5 \text{ m s}^{-1}$ , respectively; flags indicate wind speeds of  $25 \text{ m s}^{-1}$ . Surface temperature ( $^{\circ}\text{C}$ ), dewpoint temperature ( $^{\circ}\text{C}$ ), and mean sea level pressure (hPa) are also plotted in each panel.

dar datasets. This was accomplished using fixed ground targets (radio towers, water towers, etc.) of known locations (Rinehart 1978). Such nonmeteorological targets were identified in Doppler radial velocity data as a consequence of their immobility and were often also represented on USGS maps. The distance and azimuth of a target were then measured directly on the map and compared with those values obtained from the radar data, from which a correction factor could be derived. No significant offsets were found in any of the radar data.

### c. Radar and damage analysis

Images of each damage survey were overlaid directly onto corresponding radar imagery using a separate software package. This simple technique has been employed in published studies of isolated tornadic storms

and hurricanes (e.g., Wakimoto and Atkins 1996; Wakimoto and Black 1994), but its utility in studies of damaging quasi-linear convective systems has yet to be fully exploited since the installation of WSR-88Ds in the 1990s.

## 3. Wingate, Indiana: 31 May 2003

### a. Summary of event

On the evening of 31 May 2003, a line of (discrete) supercells developed over southern Wisconsin and northwestern Illinois, ahead of a warm front. The front was associated with a mature midlatitude cyclone located over southern Wisconsin at 0000 UTC on 31 May 2003 (Fig. 1a). At midlevels, strong northwesterly flow was observed over the Midwest; a jet streak (at

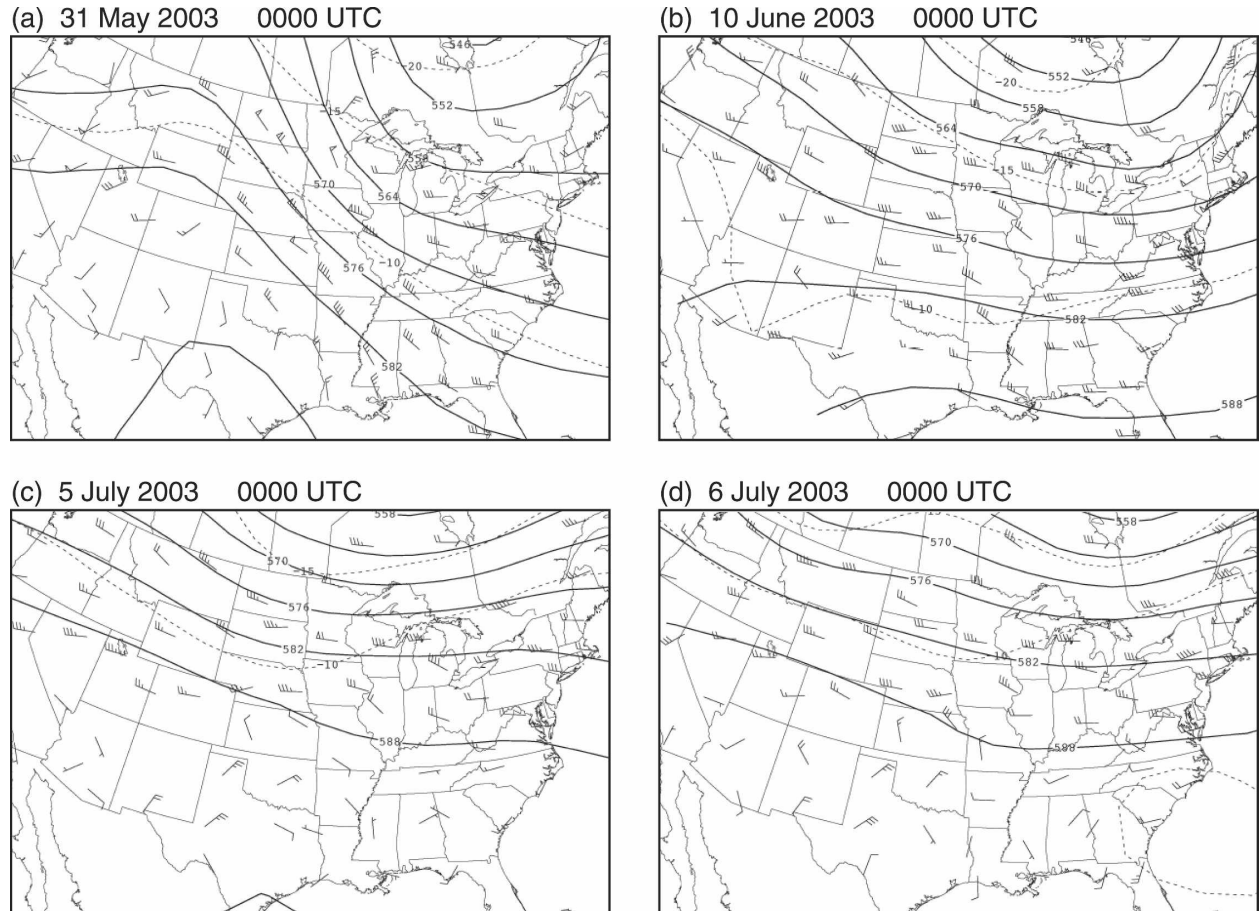


FIG. 2. Analysis of 500-hPa geopotential height [solid contours; 6-gpdm (geopotential dekameter) increment] and temperature (dashed contours; 5°C), valid 0000 UTC on (a) 31 May 2003, (b) 10 Jun 2003, (c) 5 Jul 2003, and (d) 6 Jul 2003. Full and half wind bars denote wind speeds of 5 and 2.5  $\text{m s}^{-1}$ , respectively; flags indicate wind speeds of 25  $\text{m s}^{-1}$ .

500 hPa) with wind speeds of nearly 40  $\text{m s}^{-1}$  was located over extreme southeastern Iowa and central Illinois (Fig. 2a). Hence, the meteorological conditions associated with convective initiation and subsequent MCS development were similar to the “dynamic pattern,” as described by Johns and Hirt (1987) and Johns (1993).

The 0000 UTC sounding from Lincoln, Illinois, revealed relatively low instability, with a mean-layer (ML) and most-unstable (MU) CAPE of 182 and 633  $\text{J kg}^{-1}$ , respectively (Fig. 3a). The deep-layer shear<sup>3</sup> was quite strong (33  $\text{m s}^{-1}$ ), explaining the eventual evolution of the convective storms into an intense MCS with leading stratiform precipitation region (e.g., Parker and Johnson 2004). Although a bow echo was never realized, a shallow, broad (order 5–10 km) mesovortex was observed along the leading edge of this MCS during the

period 0315:12–0335:07 UTC; according to the idealized modeling study by Weisman and Trapp (2003), the low-level shear<sup>4</sup> of 14  $\text{s}^{-1}$  (Fig. 3a) was marginally sufficient to support low-level mesovortex development.

#### b. Radar-damage analysis

This smaller-scale MCS (see Fig. 4) was not a prolific producer of nontornadic wind damage. Preliminary severe weather reports indicated that most of the wind damage resulted from tornadoes that occurred over central/northern Illinois. Nevertheless, detailed aerial and ground surveys following this event revealed a localized swath of F0-intensity wind damage approximately 15 km in length, centered about the town of Wingate, Indiana (Fig. 5a).

<sup>3</sup> Herein deep-layer shear is defined as the surface to 6-km environmental wind vector difference.

<sup>4</sup> Herein low-level shear is defined as the surface to 2-km environmental wind vector difference.



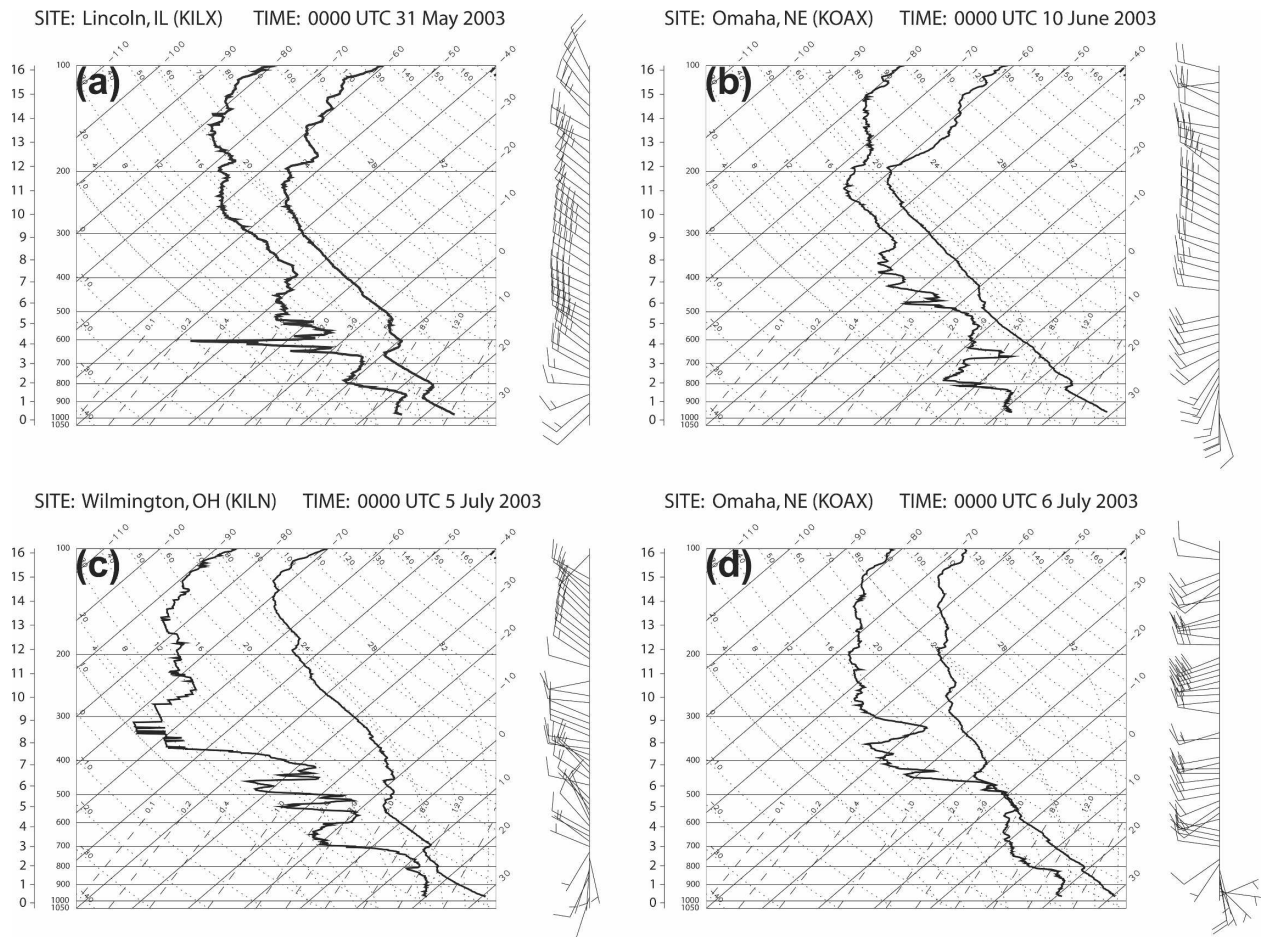


FIG. 3. Observed sounding at 0000 UTC on (a) 31 May 2003, from Lincoln, IL (KILX); (b) 10 Jun 2003, from Omaha, NE (KOAX); (c) 5 Jul 2003, from Wilmington, OH (KILN); and (d) 6 Jul 2003, from Omaha, NE (KOAX).

This damage area has been superimposed on the KIND radar reflectivity at 0329:49 UTC to establish the spatial correspondence between convective system structure and the damage locations. At this time, a shallow, broad mesovortex was observed in Doppler winds on the  $0.5^\circ$  elevation surface [approximately 1.5 km above radar level (ARL)]. This circulation persisted over five volume scans (approximately 25 min), as indicated by the track of the vortex core. Throughout its lifetime, the mesovortex showed no tendency to build upward, as its vertical depth was confined to the lowest  $\sim 1.5$  km (i.e., only seen at  $0.5^\circ$  elevation).

The onset of damaging surface winds occurred around 0324:50 UTC and persisted for three volume scans, as determined by the radar/damage superposition. During this period, winds on the southern periphery of the vortex core coincided with the observed wind damage (Fig. 5a). By 0340:06 UTC, no circulation could be detected in Doppler winds and damaging surface winds had ceased.

#### 4. Eastern Nebraska: 10 June 2003

##### a. Summary of event

This high-wind event featured a mature, extensive bow echo that evolved from two cell bow echoes, which in turn evolved from two tornadic supercells over eastern Nebraska. The synoptic-scale pattern associated with bow echo development was dominated by a developing surface low located over extreme southern South Dakota (Fig. 1b). The first area of convection initiated in an area of warm air advection associated with a west-east-oriented warm front over northeastern Nebraska, and the second area of convection initiated over east-central Nebraska, east of the dryline. A weak short-wave trough in westerly flow at 500 hPa (Fig. 2b) provided little destabilization (ML and MU CAPE of 297 and  $743 \text{ J kg}^{-1}$ , respectively, in the 0000 UTC sounding from Omaha, Nebraska; Fig. 3b), but was coupled with moist southerly flow at 850 hPa and a veering wind profile above that level to support supercell and subse-

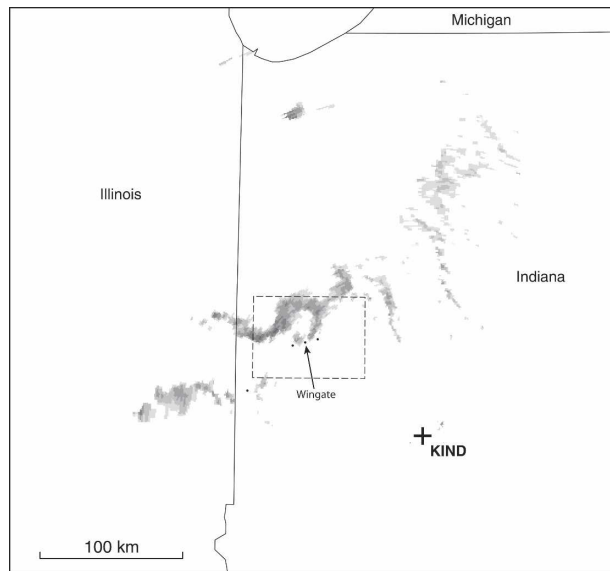


FIG. 4. Quasi-linear convective system on 31 May 2003 in Indiana. Radar reflectivity factor  $>40$  dBZ at  $\sim 0315$  UTC is shaded. Black dots indicate the locations of *Storm Data* wind reports for Indiana. Box with dashed outline encompasses the geographical area shown in the radar and damage analysis.

quent bow echo development. Indeed, this more discrete mode of convective development seems to be consistent with the relatively strong deep-layer shear of  $27 \text{ m s}^{-1}$  (Fig. 3b); the lack of significant mesovortices in the bow echoes likewise seems to be consistent with the relatively weak low-level shear of  $10 \text{ m s}^{-1}$  (e.g., Weisman and Trapp 2003).

The first supercell to bow echo evolution occurred over northeastern Nebraska around 0100 UTC, and a similar evolutionary mode was observed over east-central Nebraska around 0300 UTC. In each case, the transition process occurred rather rapidly ( $\sim 30$  min), and damaging-wind production was confined to the early formation of the bow echo. Both isolated, smaller-scale bow echoes exhibited rapid upscale growth over the next several hours as they moved southeast over extreme eastern Nebraska and southwestern Iowa.

The two smaller-scale bow echoes merged into a larger-scale bow system over southwestern Iowa, which continued to propagate toward the southeast and affected the greater St. Louis, Missouri, area around 1200 UTC. BAMEX observations (airborne Doppler radar data) documented the presence of rear inflow in the trailing stratiform precipitation region at this time; however, an aerial survey conducted post-event found that this larger-scale bow echo produced relatively minor damage as it moved through Missouri. Thus, this analysis focuses primarily on the two smaller-scale bow

echoes that did, in fact, produce damaging winds at the ground (Fig. 6).

#### b. Radar-damage analysis

##### 1) “EMERSON” BOW ECHO

Aerial and ground surveys conducted in the days immediately following this bow echo event revealed a swath of concentrated F0-intensity wind damage approximately 40 km in length (Fig. 7). The most significant wind damage occurred in Emerson, Nebraska, and surrounding areas, where severe winds caused widespread tree and power line damage, as well as minor structural damage. Property damage in these areas was estimated at \$100,000 (NCDC 2003a).

The Emerson bow echo over the period 0117:45–0147:45 UTC is of primary interest to this analysis. At 0117:45 UTC, the apex of this intense cell bow echo was nearly coincident with the first damage locations (not shown). Indeed, radial velocity data at  $0.5^\circ$  elevation from KOAX depicted a narrow RIJ that extended tens of kilometers behind the leading edge of the system. The RIJ/apex winds continued to be nearly collocated with the damage area (e.g., Fig. 5b) as the convective system exhibited pronounced bowing and propagated toward the southeast. This system was no longer producing discernable damage at 0147:45 UTC, despite its marked horseshoe shape at that time (not shown).

##### 2) “SHELBY” BOW ECHO

In east-central Nebraska, survey efforts revealed a rather narrow swath of F1-intensity wind damage approximately 10 km in length embedded within a broader distribution of F0-intensity damage locations approximately 30 km in length (Fig. 8). A secondary area of F1-intensity wind damage appeared to be the consequence of microburst winds, owing to the largely divergent damage vectors. Estimated damage in Shelby, Nebraska, alone was \$2 million (property—\$1 million, crop—\$1 million; NCDC 2003a). In addition, 22 irrigation systems were overturned throughout the damage area, several of which appeared to have been rolled over multiple times (as they were overturned in the upwind direction). It is interesting to note here that initial storm reports to the NWS mentioned only tree damage north of Shelby.

Similar to the previous analysis, the descent of the RIJ to the surface was primarily responsible for the damaging wind production in the Shelby bow echo. At 0302:59 UTC, the first F0-intensity damage locations lay underneath the apex of a 20-km-wide cell bow echo (not shown). Corresponding radial velocity data



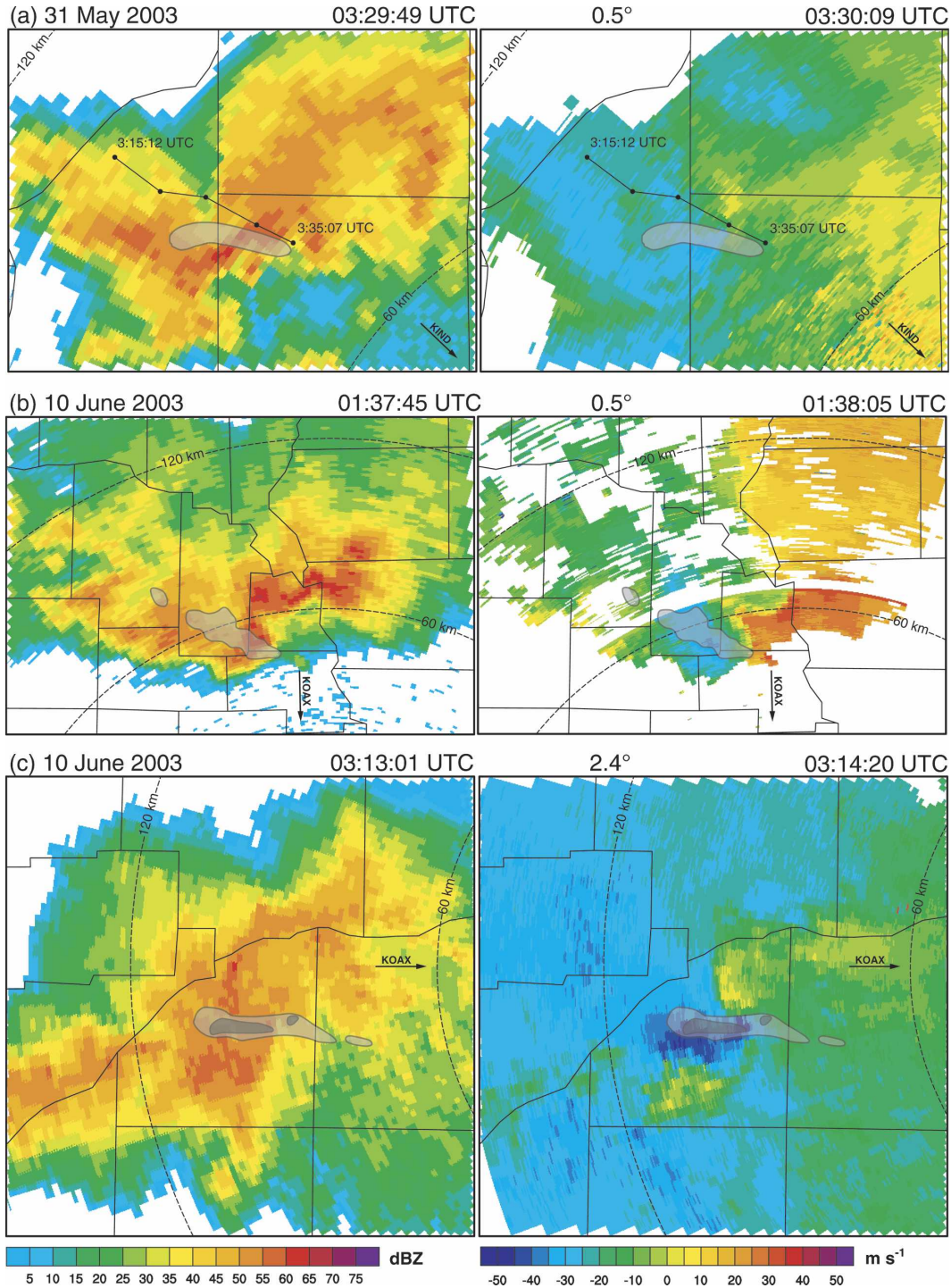


FIG. 5. Semitransparent shading of F0 (light gray) and F1 (dark gray) damage contours overlaid onto images of radar reflectivity factor and ground-relative (GR) radial velocity at (a) 0.5° elevation, from the WSR-88D KIND at 0329:49 and 0330:09 UTC 31 May 2003, respectively; (b) 0.5° elevation, from the WSR-88D KOAX at 0137:45 and 0138:05 UTC 10 Jun 2003, respectively; (c) 2.4° elevation, from the WSR-88D KOAX at 0313:01 and 0314:20 UTC 10 Jun 2003, respectively; (d) 0.5° elevation, from the WSR-88D KIWX at 2314:24 and 2314:44 UTC 4 Jul 2003, respectively; (e) 0.5° elevation, from the WSR-88D KOAX at 0524:07 and 0524:27 UTC 6 Jul 2003, respectively; and (f) 0.5° elevation, from the WSR-88D KOAX at 0554:13 and 0554:33 UTC 6 Jul 2003, respectively. Range rings are displayed at 60-km intervals. In (a), (e), and (f) the solid line shows the track of vortex core. Insets in (e) and (f) show storm-relative motion within dashed box. In (d), (e), and (f) full and half wind bars denote wind speeds of 10 and 5 m s<sup>-1</sup>, respectively.



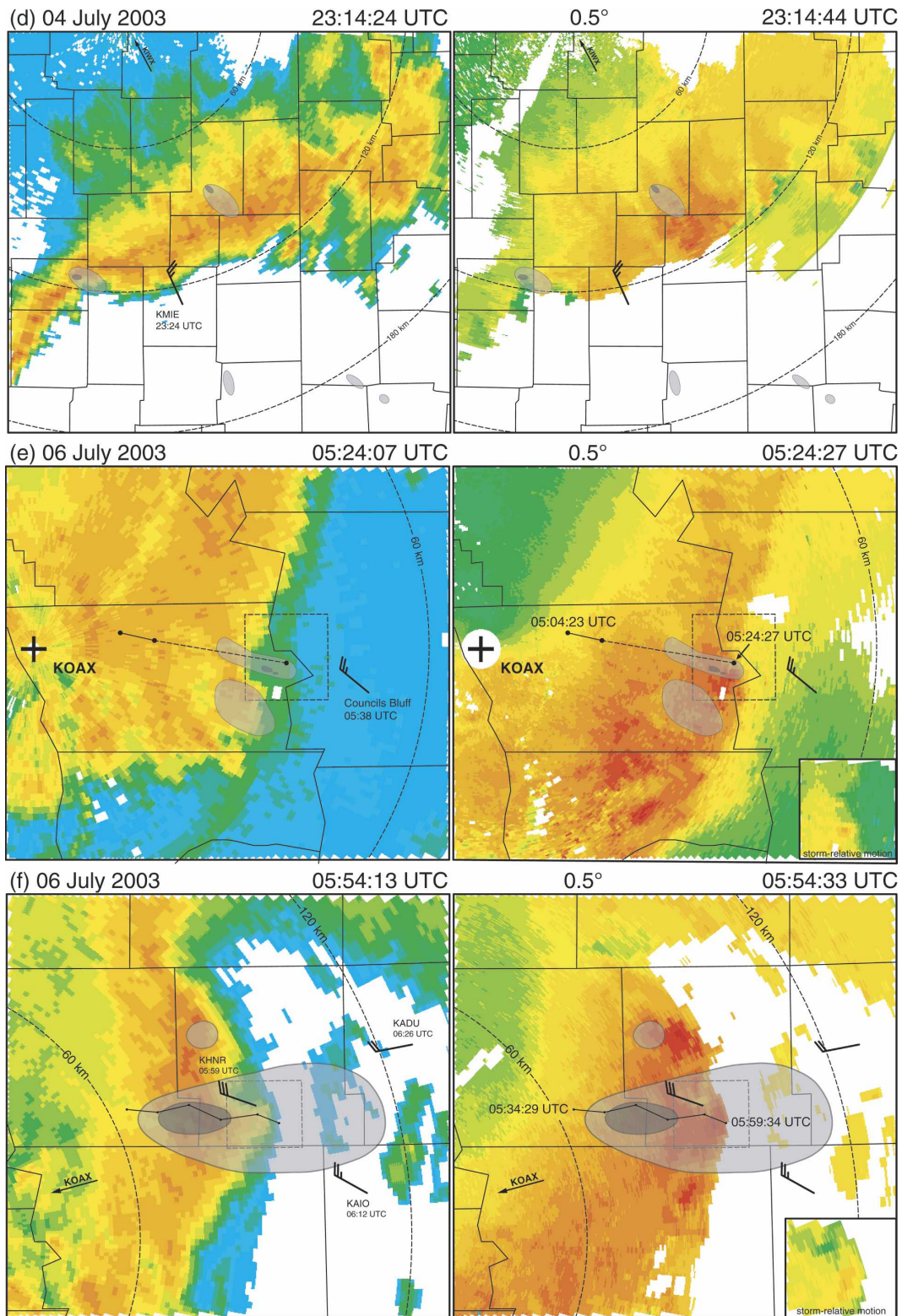


FIG. 5. (Continued)

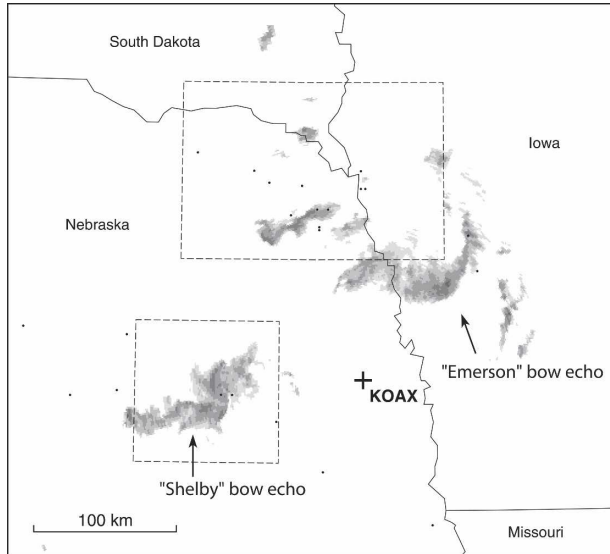


FIG. 6. As in Fig. 4, except at ~0315 UTC for the two cell bow echoes on 10 Jun 2003 in Nebraska. Because of timing differences between the two cell bow echoes, the “Emerson” bow echo lies outside of the geographical area shown in the radar and damage analysis (which implies nonseverity).

showed an intense RIJ that extended tens of kilometers rearward of the system’s leading edge. The spatial correspondence between the RIJ and damage swath continued through 0314:19 UTC (Fig. 5c).

As described by Weisman (1993), the magnitude of the RIJ may have been enhanced by midlevel line-end (or “book-end”) vortices, particularly the cyclonic member evident in Fig. 5c. Damaging surface winds

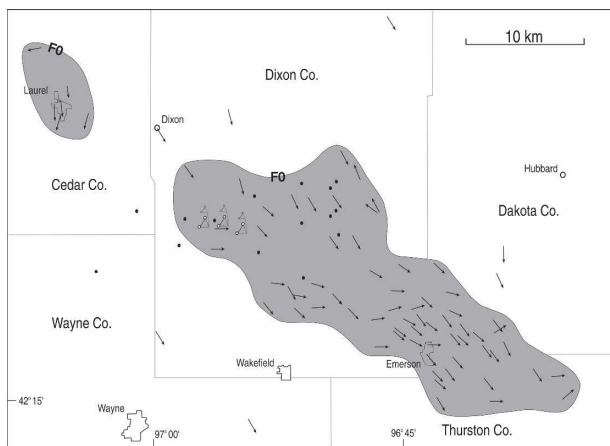


FIG. 7. Analysis of wind damage for the “Emerson” bow echo on 10 Jun 2003 over northeast Nebraska. Contours of F0 damage are lightly shaded in gray. Arrows represent “damage vectors,” and dots represent damage from which wind direction could not be inferred (see text). Triangular symbols represent damaged irrigation systems.

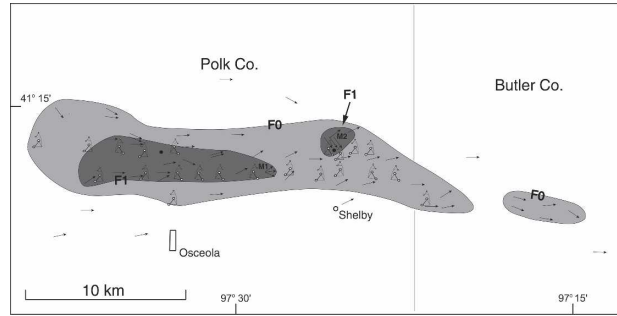


FIG. 8. As in Fig. 7, except for the “Shelby” bow echo on 10 Jun 2003 over east-central Nebraska. Contours of F1 damage are heavily shaded in gray. (M1 and M2 denote localized areas of damage caused by microbursts.)

should not be considered mesovortex-induced, given that the RIJ preceded the vortex, which formed *ahead* of the bow echo’s leading edge and distinctly north of the RIJ (see Fig. 9); thereafter, this vortex remained spatially separated from RIJ and damage path (Fig. 5c).

### 5. Indiana/Ohio: 4–5 July 2003

#### a. Summary of event

During the late afternoon hours on 4–5 July 2003, intense convective cells developed over northern Indiana, in the vicinity of a remnant surface outflow boundary. A quasi-linear convective system (depicted in Fig. 10) rapidly evolved from this convection, and then moved southeast over central Indiana and eastern Ohio, along the surface outflow boundary. Supporting the subsequent evolution of an extensive bow echo over Indiana and Ohio were meteorological conditions similar to the warm-season pattern described by Johns and Hirt (1987) and Johns (1993). A surface analysis for 0000 UTC on 5 July 2003 showed a rather benign synoptic pattern, with the eastern United States under the influence of a subtropical ridge (Fig. 1c). Surface dewpoint temperatures were in excess of 21°C over central Indiana and 18°C over eastern Ohio. Moderate northwesterly flow aloft extended from Illinois through Ohio (Fig. 2c). ML CAPE values at 0000 UTC in this region ranged from 2621 J kg<sup>-1</sup> at Lincoln, Illinois, to 1439 J kg<sup>-1</sup> at Wilmington, Ohio (Fig. 3c). Weak low-level shear of 6 m s<sup>-1</sup> was indicated in the Wilmington sounding.

#### b. Radar-damage analysis

We begin with the caveat that the following damage analysis is based only on ground survey information, since an aerial survey was not performed following this

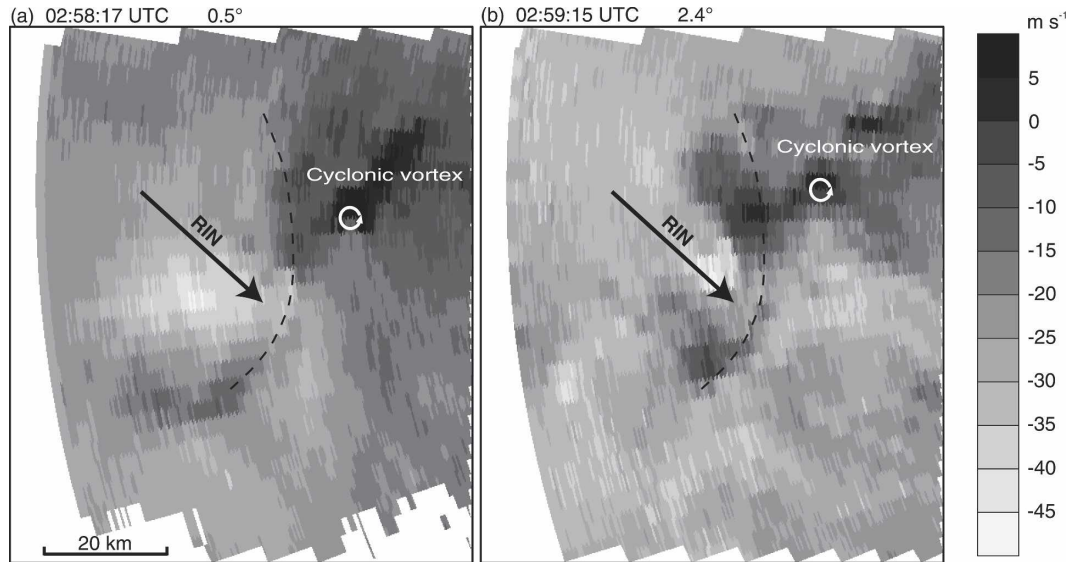


FIG. 9. Ground-relative (GR) radial velocity at (a) 0.5° elevation and (b) 2.4° elevation, from the WSR-88D KOAX at 0258:17 and 0259:15 UTC 10 Jun 2003, respectively. Dashed line represents the leading edge of the system, as inferred from the 45-dBZ radar reflectivity contour at 0.5° elevation. Arrow and accompanying text shows the location of a rear-inflow notch (RIN) at 2.4° elevation.

event. The ground survey effort, however, became complicated by a several-day sequence of convective systems over the same geographic domain affected on 4–5 July 2003. These resulted in flooding that further limited our access to rural areas, and also in additional tree damage. With this in mind, the areas of concentrated damage indicated in Fig. 11 are within the broader regions that we surveyed with a high degree of confidence. We additionally surveyed regions in and around locations of *Storm Data* reports; a lack of damage vectors in those regions implies that either (i) these were reports of *wind* and not damage or (ii) we could not verify the damage (for more discussion, see Trapp et al. 2004).

In central Indiana, survey efforts revealed two areas of relatively dense wind damage (Fig. 11). The first of these damage areas (approximately 20 km in length) was located ~40 km east-northeast of the city of Marion, near the Indiana–Ohio border. A few instances of F1 damage were observed over central Wells County. The second area was a 15-km-long swath of F0 wind damage over parts of Madison and Tipton Counties. Large trees blown over in Tipton County constituted the F1 damage.

As supported by KIWX radar data, the damage swath in Wells County can be attributed to a broad, well-defined RIJ (Fig. 5d) in a developing bow echo. Strong, albeit nondamaging winds were additionally found outside the RIJ core, as evidenced by the peak wind gust of 24 m s<sup>-1</sup> measured at Muncie, Indiana

(KMIE), following the passage of the outflow boundary (Fig. 12).

The convective system attribute that produced the damage area to the northwest of Muncie is less clear. At a range of ~120 km, the KIWX WSR-88D was clearly not sampling the low levels of the atmosphere, where damaging, near-ground winds (and associated mechanism) were present. The KIWX base reflectivity and radial velocity displays at 2314:24 and 2314:44 UTC,

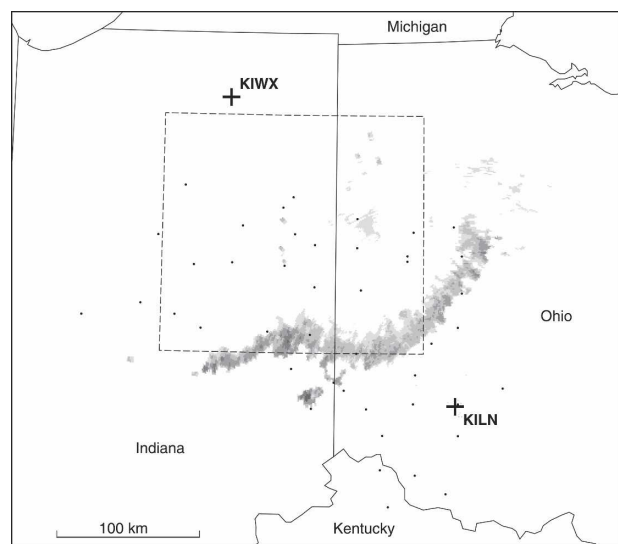


FIG. 10. As in Fig. 4, except at ~0045 UTC for the bow echo on 4–5 Jul 2003 over Indiana and Ohio.



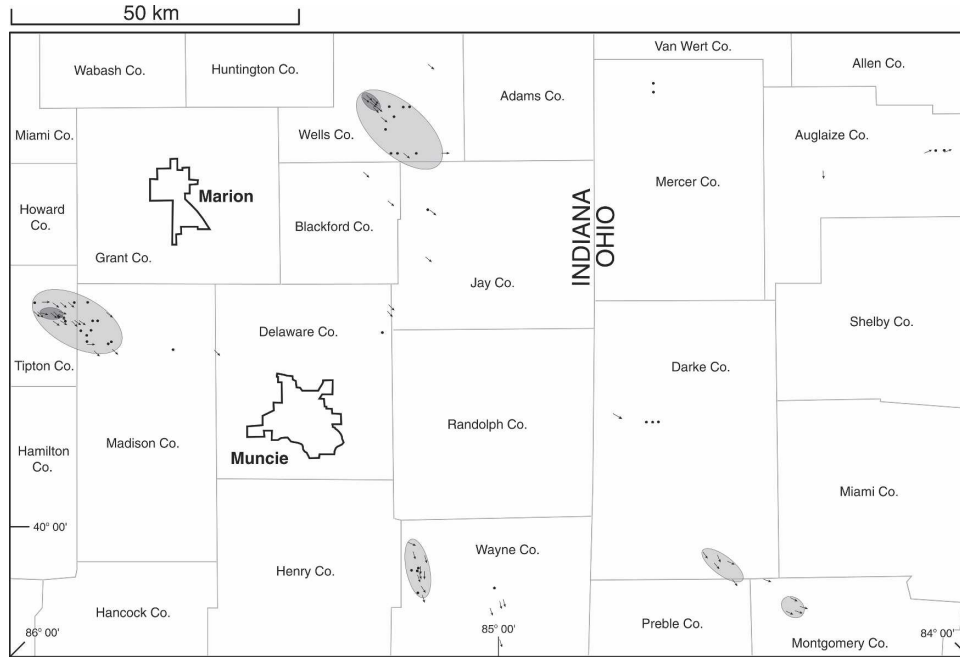


FIG. 11. As in Fig. 8, except for the bow echo on 4–5 Jul 2003 over central Indiana and eastern Ohio.

respectively, showed this damage swath clearly out of phase with the rear inflow in the expanding stratiform region. The damage area was collocated with an area of weak anticyclonic rotation, and located to the northeast of an area of weak cyclonic rotation. From a single-Doppler perspective, neither of these rotational features appeared capable of producing damaging surface winds, but it is possible that their intensities may have been undervalued as the flow inferred from the damage vectors was crossbeam. Although positioned more favorably in terms of range, KIND radar’s viewing angle also was orthogonal to the movement of the convective system structure being examined.

The relative severity of the bow echo diminished as it matured and expanded in size; survey efforts only revealed a few pockets of F0-intensity tree damage across southeast Indiana and southwest Ohio. Interestingly, radial velocity data from the KILN radar continued to indicate the presence of a broad, well-defined RIJ just behind the core of the system. Similar to the early formation of the bow echo, damaging surface winds over southeast Indiana and southwest Ohio were driven primarily by RIJ.

**6. Nebraska/Iowa: 5–6 July 2003**

*a. Summary of event*

The bow echo on 5–6 July 2003 developed from intense convection over northeastern Nebraska, on the

leading edge of a short-wave upper-level trough (visible on water vapor imagery over western Nebraska; not shown) and beneath moderately strong westerly flow ( $21 \text{ m s}^{-1}$ ) at 500 hPa (Fig. 2d). A resultant MCS moved southeastward into western Iowa, along a well-defined surface boundary (Fig. 1d). In its vicinity, the atmosphere was quite unstable (ML CAPE of  $3079 \text{ J kg}^{-1}$  in the 0000 UTC sounding from Omaha, Nebraska; Fig. 3d) and moist at low levels (surface dewpoint temperatures in excess of  $18^\circ\text{C}$  over eastern Nebraska and extreme western Iowa). Such high instability apparently

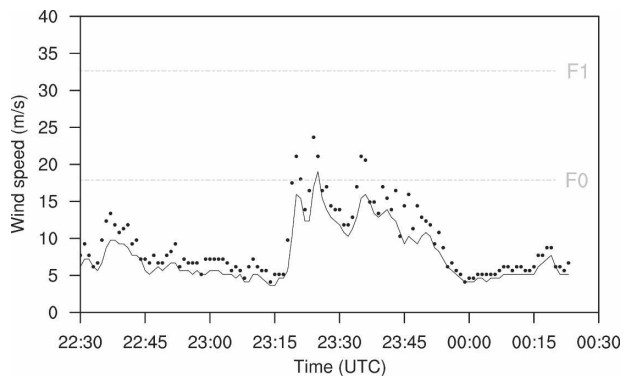


FIG. 12. Time series of 1-min wind data from Muncie, IN, Automated Surface Observing Station (ASOS) during the period 2230 UTC 4 Jul–0030 UTC 5 Jul 2003. Solid line denotes a 2-min averaged wind speed, and dots denote the maximum 5-s averaged wind speed (i.e., peak wind gust) over the past minute.

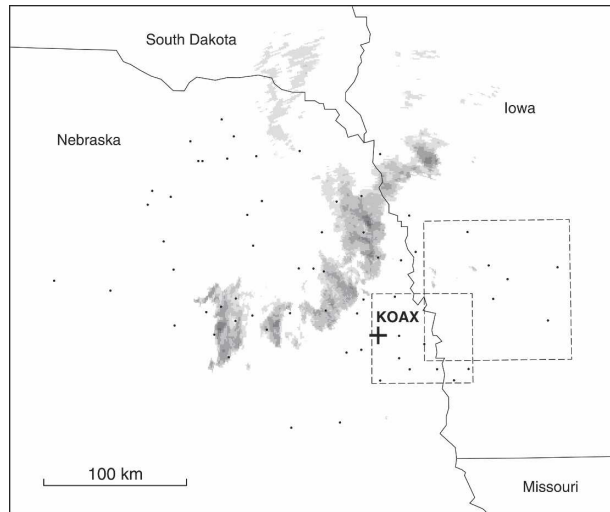


FIG. 13. As in Fig. 4, except at ~0445 UTC for the bow echo on 5–6 Jul 2003 over Nebraska and Iowa.

compensated for the relatively weak low-level shear of  $10 \text{ m s}^{-1}$ , thus allowing for the formation of significant low-level mesovortices.

This analysis examines damaging-wind production within the bow echo on 5–6 July 2003 at its mature and decaying stages. Throughout its lifetime, this convective system produced a number of high wind reports and caused widespread F0-intensity wind damage across eastern Nebraska and western Iowa (see Fig. 13). It possessed a well-defined RIJ and also a wide variety of low-level mesovortices, two of which we discuss next.

#### b. Radar-damage analysis

##### 1) OMAHA, NEBRASKA

The bow echo on 5–6 July 2003 was a prolific producer of straight-line wind damage as it moved through the Omaha metropolitan area (Fig. 14). This included a rather narrow swath (approximately 10 km in length) of F0 damage through northern sections of Omaha and a broader area of F0 damage through central Omaha. On the north side of Omaha, several F1-intensity damage locations were embedded within this broader distribution. Property damage in Douglas County, the county seat of Omaha, was estimated at \$2 million (NCDC 2003b).

During the period 0504:23–0524:27 UTC, a mesovortex was detected intermittently using KOAX radar data (Fig. 5e). Mesovortex winds at  $\sim 1 \text{ km}$  above ground level exceeded  $40 \text{ m s}^{-1}$  at 0524:27 UTC, and spatially corresponded with the only F1-intensity damage locations observed in the Omaha metropolitan area. The subsequent decay of this vortex occurred rather rapidly, as it could not be identified past 0524:27 UTC.

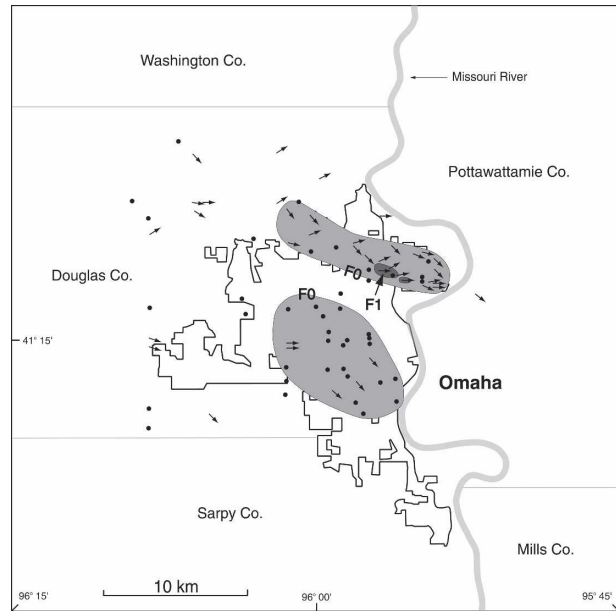


FIG. 14. As in Fig. 8, except for the bow echo on 5–6 Jul 2003 over Omaha metropolitan area.

During the same period, descending rear inflow also produced wind damage in central sections of Omaha. The Omaha NWS office reported a peak wind gust of  $28 \text{ m s}^{-1}$  as the bow system moved into Douglas County (J. Pollack 2004, personal communication), and Doppler velocity information showed that much of the county was affected by RIJ/apex winds in excess of  $30 \text{ m s}^{-1}$ . The strength of RIJ/apex winds had seemingly begun to weaken as the bow system moved into extreme eastern Iowa. At 0538 UTC, the Iowa Mesonet station at Councils Bluff, located due east of downtown Omaha, measured a peak wind gust of  $24 \text{ m s}^{-1}$  (see Fig. 5e).

##### 2) WESTERN IOWA

Aerial and ground surveys (by R. Wakimoto) over western Iowa revealed that an approximately 50-km-long swath of F0-intensity wind damage occurred across portions of Audubon, Cass, Harrison, Pottawattamie, and Shelby Counties (Fig. 5f). An approximately 15-km-long swath of F1-intensity wind damage occurred across portions of Harrison and Shelby Counties, where numerous large trees were downed by the severe winds. A secondary area of F0-intensity wind damage, attributed to microburst winds, occurred north of the primary damage area.

At 0534:09 UTC, an undulation in the reflectivity gradient along the northern end of the system revealed the presence of a second mesovortex. Corresponding

radial velocity data showed weak rotation at  $0.5^\circ$  elevation. Over the next 5 min, this second vortex rapidly intensified and deepened through midlevels, and by 0539:30 UTC, winds on the southern periphery of the vortex core were producing F0-intensity wind damage over parts of southeast Harrison County (Fig. 5f). On a time scale less than one volume scan, mesovortex winds reached peak intensity, as evidenced by the steep gradient toward the F1-intensity damage locations. F1 damage associated with this vortex continued over the duration of the next two volume scans.

Damaging winds persisted beyond this time. For example, at 0559 UTC the Iowa Mesonet station at Harlan measured a peak wind gust of  $30 \text{ m s}^{-1}$  just north of the track of the vortex core, within the primary F0-intensity damage area (see Figs. 5f and 15). Thereafter, however, rotation was no longer evident on the lowest elevation scan, possibly owing to the large distance between radar and convective-system attribute. A broad area of rotation persisted at midlevels through approximately 0615 UTC. Diminished surface winds accompanied the weakening of the vortex. The Iowa Mesonet stations at Atlantic (southeast of the primary damage area) and Audubon (northeast of the primary damage area) measured peak wind gusts of 25 and  $20 \text{ m s}^{-1}$  at 0612 and 0626 UTC, respectively (see Fig. 5f).

## 7. Summary and discussion

A simple technique has been employed to investigate damaging-wind production in bow echoes, whereby documented locations of damage were overlaid directly onto radar images. The results of the present study provide clear observational evidence that, in addition to descending rear inflow at the bow echo apex, low-level mesovortices within bow echoes can produce damaging straight-line winds at the ground. The various bow echo events are summarized as follows.

In four of the five damage analyses presented as part of this study, a midlevel RIJ was present in the trailing stratiform precipitation region of the bow-shaped convective system. Largely, descending rear inflow at the bow echo apex produced F0-intensity wind damage. The squall line bow echo on 4–5 July 2003, with a horizontal scale in excess of 100 km, produced only localized F0 damage areas with embedded F1-intensity wind damage, as revealed by ground surveys. In the case of the bow echo on 5–6 July 2003, the RIJ produced widespread F0-intensity wind damage across eastern Nebraska and western Iowa; more intense wind damage was associated with low-level mesovortices.

Damage analyses of the “Emerson” and “Shelby”

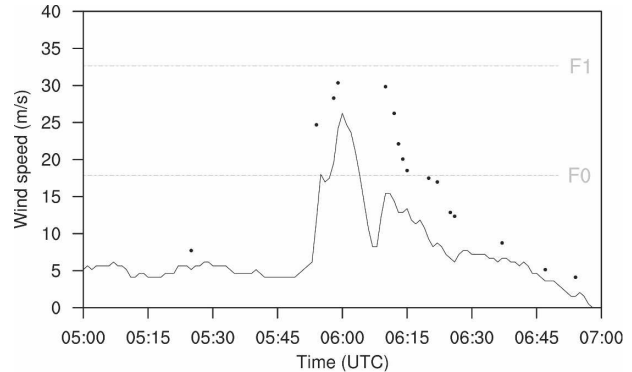


FIG. 15. As in Fig. 12, except from Harlan, IA, Automated Weather Observing Station (AWOS) during the period 0500–0700 UTC on 6 Jul 2003.

bow echoes on 10 June 2003 suggest a possible relationship between the horizontal scale of a bow echo and the strength of the RIJ. Both of these systems rapidly evolved from tornadic supercells into intense cell bow echoes. While damaging-wind production was confined to the formative stages of these systems, the distributions of damage locations were rather dense. Further, the “Shelby” bow echo produced a narrow swath of F1-intensity wind damage approximately 10 km in length.

The results of this study, as well as a parallel investigation of a squall-line bow echo that caused considerable damage in southwestern Illinois on 10 June 2003 (Atkins et al. 2005), have substantiated the mesovortex–damaging-wind paradigm put forth by Trapp and Weisman (2003). When present, low-level mesovortices in BAMEX bow echo events were associated with the most intense wind damage. The MCS on 31 May 2003 over central Indiana lacked an intense RIJ, but strong surface winds (F0 intensity) were driven for a brief time (approximately three volume scans) by a shallow, broad mesovortex located in the active leading-line convection. Otherwise, the parent system was not associated with severe winds as it continued to propagate across central Indiana, as gauged by *Storm Data* reports.

The bow echo on 5–6 July 2003 produced widespread F0-intensity wind damage across eastern Nebraska and western Iowa, but the most damaging straight-line winds occurred in association with two mesovortices in the bowing system. Notably, the second vortex produced an approximately 15-km-long swath of F1-intensity wind damage (over western Iowa), which was embedded within a primary (F0 intensity) damage area over 50 km in length!

While the present study has evidenced the severe weather potential of low-level mesovortices within bow



echoes, the question remains whether damaging mesovortex winds can be anticipated in an operational setting. In the present study, the development of these mesovortices occurred rather rapidly (a couple of radar volume scans) and hence would limit warning lead time. It should be noted that Atkins et al. (2004) found tornadic mesovortices within the quasi-linear convective system (QLCS) on 29 June 1998 (over Iowa and Illinois) to be stronger and longer-lived than nontornadic mesovortices. Thus, it would seem that the formulation of a definitive means by which to distinguish severe/nonsevere mesovortices awaits examination of mesovortex structure within future bow echo events.

*Acknowledgments.* The research results presented herein were supported by the National Science Foundation under Grants ATM-023344 (RJT and DMW) and ATM-0233178 (NTA). We are grateful to Dr. Roger Wakimoto for his damage survey information of the 5–6 July 2003 bow echo event, and also to Mr. Jon Chamberlain for his assistance in the surveys of several other events during BAMEX. The comments and suggestions of the three anonymous reviewers were helpful in clarifying many parts of the manuscript.

#### REFERENCES

- Atkins, N. T., J. M. Arnott, R. W. Przybylinski, R. A. Wolf, and B. D. Ketcham, 2004: Vortex structure and evolution within bow echoes. Part I: Single-Doppler and damage analysis of the 29 June 1998 derecho. *Mon. Wea. Rev.*, **132**, 2224–2242.
- , C. S. Bouchard, R. W. Przybylinski, R. J. Trapp, and G. Schmocker, 2005: Damaging surface wind mechanisms within the 10 June 2003 Saint Louis bow echo during BAMEX. *Mon. Wea. Rev.*, **133**, 2275–2296.
- Cotton, W. R., R. McAnelly, and C. Wolff, 2003: Mesoscale vortices and mesocyclones as precursors to derechos. Preprints, *10th Conf. on Mesoscale Processes*, Seattle, WA, Amer. Meteor. Soc., CD-ROM, 4.3.
- Davis, C., and Coauthors, 2004: The Bow Echo and MCV Experiment (BAMEX): Observations and opportunities. *Bull. Amer. Meteor. Soc.*, **85**, 1075–1093.
- Forbes, G. S., and R. M. Wakimoto, 1983: A concentrated outbreak of tornadoes, downbursts, and microbursts, and implications regarding vortex classification. *Mon. Wea. Rev.*, **111**, 220–235.
- Fujita, T. T., 1978: Manual of downburst identification for project Nimrod. Satellite and Mesometeorology Research Paper 156, Dept. of Geophysical Sciences, University of Chicago, 104 pp.
- , 1981: Tornadoes and downbursts in the context of generalized planetary scales. *J. Atmos. Sci.*, **38**, 1511–1524.
- Funk, T. W., K. E. Darmofal, J. D. Kirkpatrick, V. L. Dewald, R. W. Przybylinski, G. K. Schmocker, and Y.-J. Lin, 1999: Storm reflectivity and mesocyclone evolution associated with the 15 April 1994 squall line over Kentucky and southern Indiana. *Wea. Forecasting*, **14**, 976–993.
- Hamilton, R. E., 1970: Use of detailed intensity radar data in mesoscale surface analysis of the 4 July 1969 storm in Ohio. Preprints, *14th Conf. on Radar Meteorology*, Tucson, AZ, Amer. Meteor. Soc., 339–342.
- Johns, R. H., 1993: Meteorological conditions associated with bow echo development in convective storms. *Wea. Forecasting*, **8**, 294–299.
- , and W. D. Hirt, 1987: Derechos: Widespread convectively induced windstorms. *Wea. Forecasting*, **2**, 32–49.
- Jorgensen, D. P., and B. F. Smull, 1993: Mesovortex circulations seen by airborne Doppler radar within a bow-echo mesoscale convective system. *Bull. Amer. Meteor. Soc.*, **74**, 2146–2157.
- Lakshmanan, V., 2002: WDSS-II: An extensible, multi-source meteorological algorithm development interface. Preprints, *21st Conf. on Severe Local Storms*, San Antonio, TX, Amer. Meteor. Soc., 134–137.
- Lee, W. C., R. M. Wakimoto, and R. E. Carbone, 1992: The evolution and structure of a “bow-echo-microburst” event. Part II: The bow echo. *Mon. Wea. Rev.*, **120**, 2211–2225.
- Miller, D. J., and R. H. Johns, 2000: A detailed look at extreme wind damage in derecho events. Preprints, *20th Conf. on Severe Local Storms*, Orlando, FL, Amer. Meteor. Soc., 52–55.
- NCDC, 2003a: *Storm Data*. Vol. 45, No. 6, 385 pp. [Available from National Climatic Data Center, 151 Patton Ave., Asheville, NC 28801-5001.]
- , 2003b: *Storm Data*. Vol. 45, No. 7, 477 pp. [Available from National Climatic Data Center, 151 Patton Ave., Asheville, NC 28801-5001.]
- Nolen, R. H., 1959: A radar pattern associated with tornadoes. *Bull. Amer. Meteor. Soc.*, **40**, 277–279.
- Oye, R., C. Mueller, and S. Smith, 1995: Software for radar translation, visualization, editing, and interpolation. Preprints, *29th Conf. on Radar Meteorology*, Vail, CO, Amer. Meteor. Soc., 359–361.
- Parker, M. D., and R. H. Johnson, 2004: Structures and dynamics of quasi-2D mesoscale convective systems. *J. Atmos. Sci.*, **61**, 545–567.
- Przybylinski, R. W., G. K. Schmocker, and Y.-J. Lin, 2000: A study of storm and vortex morphology during the “intensifying stage” of severe wind mesoscale convective systems. Preprints, *20th Conf. on Severe Local Storms*, Orlando, FL, Amer. Meteor. Soc., 173–176.
- Rinehart, R. E., 1978: On the use of ground targets for radar reflectivity factor calibration checks. *J. Appl. Meteor.*, **17**, 1342–1350.
- Schmocker, G. K., R. W. Przybylinski, and E. N. Rasmussen, 2000: The severe bow echo event of 14 June 1998 over the mid-Mississippi Valley region: A case of vortex development near the intersection of a preexisting boundary and a convective line. Preprints, *20th Conf. on Severe Local Storms*, Orlando, FL, Amer. Meteor. Soc., 169–172.
- Smull, B. F., and R. A. Houze Jr., 1987: Rear inflow in squall lines with trailing stratiform precipitation. *Mon. Wea. Rev.*, **115**, 2869–2889.
- Stumpf, G. J., A. Witt, E. D. Mitchell, P. L. Spencer, J. T. Johnson, M. D. Eilts, K. W. Thomas, and D. W. Burgess, 1998: The National Severe Storms Laboratory mesocyclone detection algorithm for the WSR-88D. *Wea. Forecasting*, **13**, 304–326.
- , T. Smith, and A. Gerard, 2002: The multiple-radar severe storm analysis program for WDSS-II. Preprints, *21st Conf. on Severe Local Storms*, San Antonio, TX, Amer. Meteor. Soc., 138–141.
- Trapp, R. J., and M. L. Weisman, 2003: Low-level mesovortices

- within squall lines and bow echoes. Part II: Their genesis and implications. *Mon. Wea. Rev.*, **131**, 2804–2823.
- , D. M. Wheatley, N. T. Atkins, and R. P. Przybylinski, 2004: Some caution on the use of wind reports in post-event assessment and research. Preprints, *22d Conf. on Severe Local Storms*, Hyannis, MA, Amer. Meteor. Soc., CD-ROM, P3.7.
- Wakimoto, R. M., and P. G. Black, 1994: Damage survey of Hurricane Andrew and its relationship to the eyewall. *Bull. Amer. Meteor. Soc.*, **75**, 189–200.
- , and N. T. Atkins, 1996: Observations on the origins of rotation: The Newcastle tornado during VORTEX 94. *Mon. Wea. Rev.*, **124**, 384–407.
- Weisman, M. L., 1993: The genesis of severe, long-lived bow echoes. *J. Atmos. Sci.*, **50**, 645–670.
- , and R. J. Trapp, 2003: Low-level mesovortices within squall lines and bow echoes. Part I: Overview and dependence on environmental shear. *Mon. Wea. Rev.*, **131**, 2779–2803.
- Witt, A., M. D. Eilts, G. J. Stumpf, E. D. Mitchell, J. T. Johnson, and K. W. Thomas, 1998: Evaluating the performance of the WSR-88D severe storm detection algorithms. *Wea. Forecasting*, **13**, 513–518.
- Wolf, R. A., 2000: Characteristics of circulations associated with the 29 June 1998 derecho in eastern Iowa. Preprints, *20th Conf. on Severe Local Storms*, Orlando, FL, Amer. Meteor. Soc., 56–59.